CHEMISTRY
A EUROPEAN JOURNAL

DOI: 10.1002/chem.200401334

Synthesis and Characterization of Heterometallic Clusters (Ir_2Rh, Ir_2W, Rh_3) Containing 1,2-Dicarba-*closo*-dodecaborane(12)-1,2-dithiolate Chelate Ligands, $[(B_{10}H_{10})C_2S_2]^{2-}$

Jian-Qiang Wang,[a] Shuyi Cai,[a] Guo-Xin Jin,*[a] Lin-Hong Weng,[a] and Max Herberhold[b]

Abstract: The 16-electron half-sandwich complex $[Cp^*Ir\{S_2C_2(B_{10}H_{10})\}]$ ($Cp^* = \eta^5$-C_5Me_5) (**1a**) reacts with $[\{Rh(cod)(\mu\text{-}Cl)\}_2]$ (cod = cycloocta-1,5-diene, C_8H_{12}) in different molar ratios to give three products, $[\{Cp^*Ir[S_2C_2(B_{10}H_9)]\}Rh(cod)]$ (**2**), *trans*-$[\{Cp^*Ir[S_2C_2(B_{10}H_9)]\}Rh\{[S_2C_2(B_{10}H_{10})]IrCp^*\}]$ (**3**), and $[Rh_2(cod)_2\{(\mu\text{-}SH)(\mu\text{-}SC)(CH)(B_{10}H_{10})\}]$ (**4**). Complex **3** contains an Ir_2Rh backbone with two different Ir–Rh bonds (3.003(3) and 2.685(3) Å). The dinuclear complex **2** reacts with the mononuclear 16-electron complex **1a** to give **3** in refluxing toluene. Reaction of **1a** with $[W(CO)_3(py)_3]$ ($py = C_5H_5N$) in the presence of $BF_3{\cdot}EtO_2$ leads to the trinuclear cluster $[\{Cp^*Ir[S_2C_2(B_{10}H_{10})]\}_2W(CO)_2]$ (**5**) together with $[\{Cp^*Ir(CO)[S_2C_2(B_{10}H_{10})]\}W(CO)_5]$ (**6**), and $[Cp^*Ir(CO)\{S_2C_2(B_{10}H_{10})\}]$ (**7**). Analogous reactions of $[Cp^*Rh\{S_2C_2(B_{10}H_{10})\}]$ (**1b**) with $[\{Rh(cod)(\mu\text{-}Cl)\}_2]$ were investigated and two complexes *cis*-$[\{Cp^*Rh[S_2C_2(B_{10}H_{10})]\}_2Rh]$ (**8**) and *trans*-$[\{Cp^*Rh[S_2C_2(B_{10}H_{10})]\}_2Rh]$ (**9**) were obtained. In refluxing THF solution, the cisoid **8** is converted in more than 95% yield to the transoid **9**. All new complexes **2**–**9** were characterized by NMR spectroscopy (^1H, ^{11}B NMR) and X-ray diffraction structural analyses are reported for complexes **2**–**5, 8**, and **9**.

Keywords: carboranes · dithiolato ligands · iridium · rhodium · structure elucidation

Introduction

During the last decade, a series of mononuclear 16-electron Cp* half-sandwich complexes of Co, Rh, Ir have been prepared that contain a bidentate, chelating 1,2-dicarba-*closo*-dodecaborane(12)-1,2-dichalcogenolate ligand $[(B_{10}H_{10})C_2E_2]^{2-}$ (E = S, Se).[1] These complexes exhibit a rich coordination chemistry, due to both their unsaturation at the metal atom and the bridging or chelating properties of the sulfur or selenium atoms respectively.[2] Although addition reactions at the metal atom have readily been accomplished,[3] and the formation of a metal-to-boron bond and/or substitution of the carborane cage in the positions of B(3)/B(6) have also been achieved,[4] the formation of heteronuclear metal–metal bonds from the half-sandwich complexes with the support of an ancillary dithiolate-*o*-carborane ligand has received only scant attention. In a previous paper, we have reported the synthesis of heterotrinuclear clusters with bridging diselenolate-*o*-carborane ligands, such as *cis*-$[\{Cp^*Ir[Se_2C_2(B_{10}H_{10})]\}_2Rh]$, $[\{Cp^*Ir[Se_2C_2(B_{10}H_{10})]\}_2Mo(CO)_2]$, $[\{Cp^*Ir[Se_2C_2(B_{10}H_{10})]\}_2W(CO)_2]$, which contain hetero metal–metal bonds. They were obtained from the reactions of the 16-electron complex $[Cp^*Ir\{Se_2C_2(B_{10}H_{10})\}]$ with $[\{Rh(cod)(\mu\text{-}Cl)\}_2]$, $[Mo(CO)_3(NC_5H_5)_3]$, $[W(CO)_3(NC_5H_5)_3]$, respectively.[5] Moreover, *cis*-$[\{Cp^*Ir[Se_2C_2(B_{10}H_{10})]\}_2Rh]$ was found to be thermally converted into *trans*-$[\{Cp^*Ir[Se_2C_2(B_{10}H_9)]\}Rh\{[Se_2C_2(B_{10}H_{10})]IrCp^*\}]$ by generation of an additional Ir–B bond.

Aiming at the development of versatile and rational methods for the synthesis of heterometallic clusters bridged by dichalcogenolate-o-carborane ligands, we have extended our study to include the *o*-carborane-1,2-dithiolate complexes $[Cp^*M\{S_2C_2(B_{10}H_{10})\}]$ (M = Ir, **1a**; Rh, **1b**). Herein, we report the synthesis of the unprecedented dinuclear complex $[\{Cp^*Ir[S_2C_2(B_{10}H_9)]\}Rh(cod)]$ (**2**), the mixed-valence

[a] Dr. J.-Q. Wang, S. Cai, Prof. Dr. G.-X. Jin, Prof. Dr. L.-H. Weng
Laboratory of Molecular Catalysis and Innovative Material
Department of Chemistry, Fudan University
Shanghai 200433 (P. R. China)
Fax: (+86) 21-6564-3776
E-mail: gxjin@fudan.edu.cn

[b] Prof. Dr. M. Herberhold
Anorganische Chemie II, Universität Bayreuth
95440 Bayreuth (Germany)

trinuclear cluster *trans*-[{Cp*Ir-[$S_2C_2(B_{10}H_9)$]}Rh{[$S_2C_2(B_{10}H_{10})$]-IrCp*}] (**3**), [$Rh_2(cod)_2$-{S(SH)C(CH)($B_{10}H_{10}$)}] (**4**), and [{Cp*Ir[$S_2C_2(B_{10}H_{10})$]}$_2$W(CO)$_2$] (**5**). We have also studied the similar behavior of the comparable rhodium complexes *cis*-[{Cp*Rh[$S_2C_2(B_{10}H_{10})$]}$_2$Rh] (**8**), *trans*-[{Cp*Rh[$S_2C_2(B_{10}H_{10})$]}$_2$-Rh] (**9**). All products were-obtained from the half-sandwich dithiolate complexes [Cp*M{$S_2C_2(B_{10}H_{10})$}] (M = Ir, **1a**; Rh, **1b**) (Cp* = η^5-C_5Me_5), by reactions with [{Rh(cod)(μ-Cl)}$_2$] (cod = cycloocta-1,5-diene, C_8H_{12}), or [$W(CO)_3(NC_5H_5)_3$], respectively.

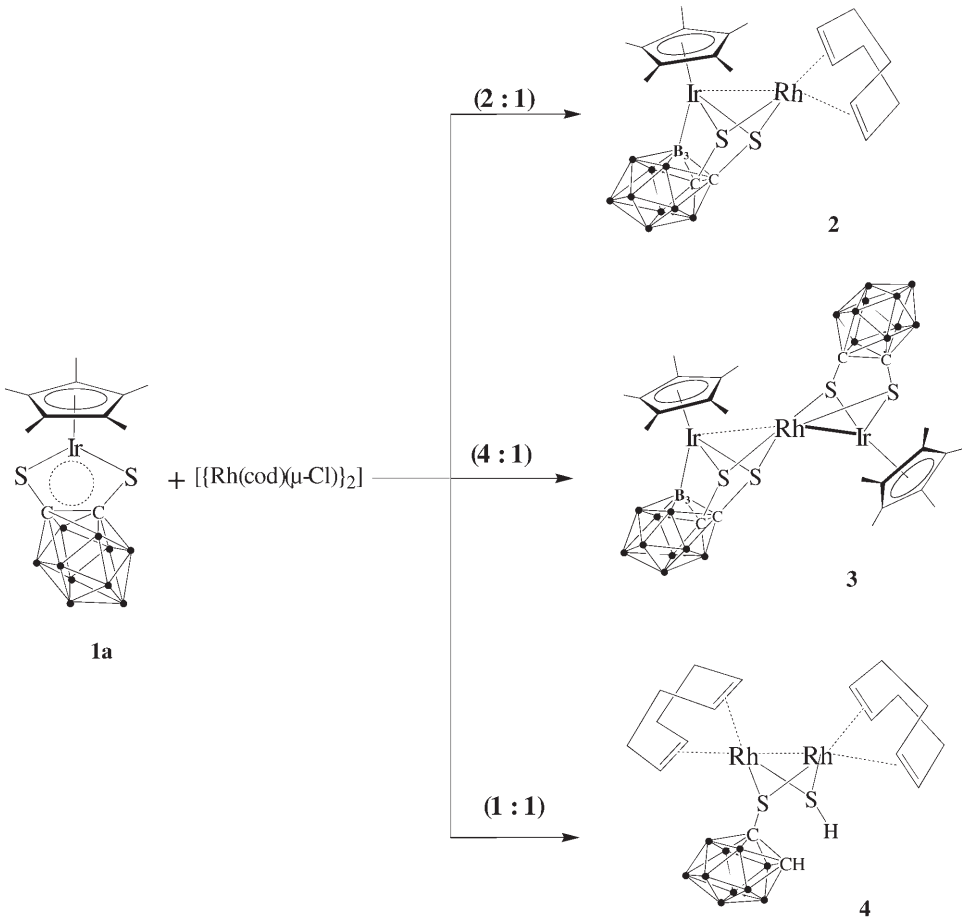

Scheme 1. Reaction of iridium complex **1a** with [{Rh(cod)(μ-Cl)}$_2$] to give complexes **2**–**4**.

Results and Discussion

Synthesis and reactivity of {Cp*Ir[$S_2C_2(B_{10}H_9)$]}Rh(cod) (2): The 16-electron complex **1a**, which is easily synthesized from the half-sandwich iridium dichloride complex [{Cp*IrCl-(μ-Cl)}$_2$] with dilithium 1,2-dicarba-*closo*-dodecaborane(12)-1,2-dithiolate,[6] was allowed to react with [{Rh(cod)(μ-Cl)}$_2$] in the molar ratio 2:1. When the mixture was refluxed in toluene for 48 h, red crystals of [{Cp*Ir[$S_2C_2(B_{10}H_9)$]}Rh(cod)] (**2**) were isolated in 61 % yield (Scheme 1). The molecule **2** contains an Ir–B bond, as indicated by the appearance of Ir↔B resonances in the ^{11}B NMR spectrum at $\delta = -19$ ppm.[7] This kind of metal-induced B–H activation reaction has also been found in other cases.[4,8] The molecular structure of **2** has been determined by X-ray diffraction methods using a single crystal, obtained by slow diffusion of hexane into a concentrated solution of the complex in toluene at low temperature.

The molecule **2** has crystallographically imposed C_s symmetry with the two metal atoms occupying special positions in the symmetry plane (Figure 1). The Ir–Rh core is capped in a nearly symmetrical manner by two μ_3-sulfido ligands. The geometry around the rhodium atom is square-planar, with the metal atom bonded to both sulfido groups and to the two olefinic bonds of an η^4-cyclo-octa-1,5-diene ligand. The iridium center adopts a three-legged piano stool arrangement by coordination with the two sulfur atoms and the boron atom, apart from the η^5-cyclopentadienyl ligand, if not considering the Ir–Rh bond. The *o*-carborane-1,2-dithiolate bridge combines a [Cp*Ir] and a [Rh(cod)] fragment. The iridadithiolate heterocycle (Ir(1)-S(1)-C(1)-C(1A)-S(2A)) is bent with a dihedral angle at the S(1)···S(1A) vector of 142.5° due to the formation of the Ir–B bond (2.096(11) Å). Selected bond lengths and angles are presented in Table 1. The long Ir(1)–Rh(1) separation (3.0596(12) Å) and the formation of the Ir(1)–B(3) bond in-

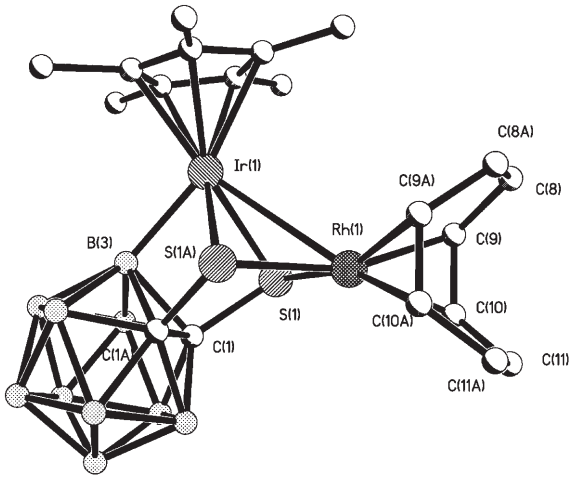

Figure 1. Molecular structure of complex **2** with atom labelling, all hydrogen atoms are omitted for clarity.

Table 1. Selected bond lengths [Å] and angles [°] for **2**.

Ir(1)–Rh(1)	3.0596(12)	Ir(1)–B(3)	2.096(11)
Ir(1)–S(1)	2.4382(15)	Rh(1)–S(1)	2.3219(15)
Rh(1)–C(9)	2.142(6)	Rh(1)–C(10)	2.138(6)
S(1)–C(1)	1.800(5)	C(1)–C(1A)	1.655(11)
Ir(1)-B(3)-C(1)	98.5(5)	Ir(1)-S(1)-C(1)	85.47(18)
Ir(1)-Rh(1)-S(1)	51.69(4)	Ir(1)-S(1)-Rh(1)	79.95(5)
Rh(1)-Ir(1)-S(1)	48.35(4)	Rh(1)-S(1)-C(1)	106.97(19)

dicate that a weak bonding interaction exists between the two metal atoms. The bond lengths and angles of the cyclo-octa-1,5-diene ligand are as expected, and the Rh–C_{alkene} bond lengths (2.138(6)–2.142(6) Å) are in the expected range for a Rh^{I} metal center coordinated to an alkene.[9]

An investigation of the reactivity of complex **2** revealed that the trinuclear complex *trans*-[{Cp*Ir[$S_2C_2(B_{10}H_9)$]}Rh{[$S_2C_2(B_{10}H_{10})$]IrCp*}] (**3**) can be constructed in a systematic way. When a mixture of complex **2** and **1a** in toluene was refluxed, we obtained complex **3** in approximately 60% yield (Scheme 2). The complex **3** can also be directly obtained through the reaction of **1a** with [{Rh(cod)(μ-Cl)}$_2$] in the molar ratio of 4:1, similar to the synthesis of *trans*-[{Cp*Ir[$Se_2C_2(B_{10}H_9)$]}Rh{[$Se_2C_2(B_{10}H_{10})$]IrCp*}].[5] We confirmed the identity of complex **3** by NMR, IR, and X-ray diffraction studies.

In the trinuclear complex **3**, only one of the ancillary *o*-carborane groups contains the Ir–B bond that is present in **2**. The molecule **3** is therefore asymmetric, as confirmed by the ^{1}H NMR spectrum with two singlet resonances of the Cp* rings at $\delta = 2.11$ and 2.19 ppm. In addition to the NMR data, the X-ray structural analysis of complex **3** verifies the presence of the Ir–B bond and the two nonequivalent Ir–Rh bonds (selected structural data are given in Table 2).

The molecular structure of molecule **3** shown in Figure 2 shows a slightly bent (173.85(10)°) Ir-Rh-Ir backbone. The two iridium atoms have retained their Cp* rings. The Rh center is six-coordinate with distorted octahedral geometry. The Rh atom and the four sulfide ligand atoms are almost coplanar (Rh(1), S(1), S(2), S(3), S(4) plane with maximal deviation of 0.0022 Å). The Ir(1) atom takes a three-legged piano stool configuration with two four-membered metallacyclic Ir-S-C-B rings. This is due to the cyclometalation of the coordinated dithiolate ligand at the iridium metal

Table 2. Selected bond lengths [Å] and angles [°] for **3**.

Ir(1)–S(1)	2.433(7)	Ir(1)–S(2)	2.407(7)
Ir(1)–B(3)	2.16(3)	C(1)–C(2)	1.55(3)
Rh(1)–Ir(1)	3.003(3)	Rh(1)–Ir(2)	2.685(3)
Rh(1)–S(1)	2.257(8)	Rh(1)–S(2)	2.244(10)
Rh(1)–S(3)	2.372(8)	Rh(1)–S(4)	2.375(8)
Ir(2)–S(3)	2.333(6)	Ir(2)–S(4)	2.319(6)
Ir(1)-Rh(1)-Ir(2)	173.85(10)	Ir(1)-S(1)-Rh(1)	79.5(2)
Ir(1)-S(2)-Rh(1)	80.3(2)	Ir(1)-B(3)-C(1)	99.7(14)
Ir(1)-B(3)-C(2)	100.0(14)	Ir(1)-S(1)-C(1)	86.6(8)
Ir(1)-S(2)-C(2)	86.9(7)	S(1)-Ir(1)-S(2)	77.2(2)
Rh(1)-Ir(1)-S(1)	47.6(2)	Rh(1)-S(1)-Ir(1)	79.5(2)
S(1)-Rh(1)-S(2)	84.3(3)	S(3)-Rh(1)-S(4)	79.8(3)
Ir(2)-S(3)-Rh(1)	69.59(18)	Ir(2)-S(4)-Rh(1)	69.8(2)
Ir(2)-S(3)-C(11)	102.8(8)	Ir(2)-S(4)-C(12)	103.1(8)

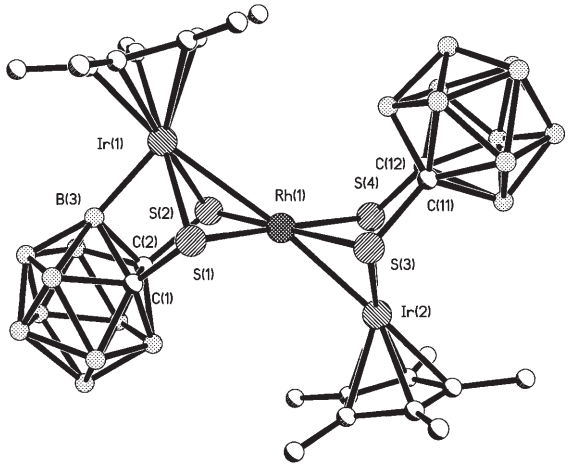

Figure 2. Molecular structure of complex **3** with atom labelling, all hydrogen atoms are omitted for clarity.

center. The Ir(1)–B(3) bond length (2.16(3) Å) in **3** is longer than that in molecule **2** (2.096(11) Å), and the Ir(1)–Rh(1) bond (3.003(3) Å) is longer than the Ir(2)–Rh(1) bond (2.685(3) Å), and this can be rationalized by the fact that the formal oxidation ("valence") state is +3 for Ir(1) and +2 for Ir(2). Although only a weak interaction can be assumed for the Ir(1)–Rh(1) bond, the Ir(2)–Rh(1) bond length of 2.685(3) Å lies in the expected range for a metal–

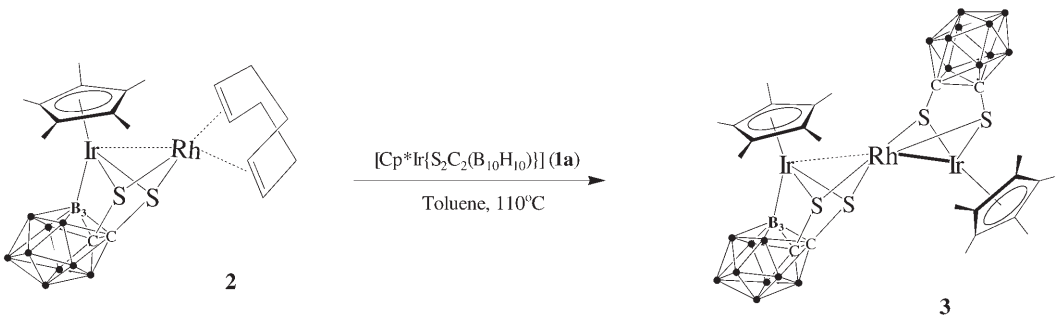

Scheme 2. The conversion of complex **2** to **3**.

metal bond. Similar Rh–Ir separations were found in $[Cp^{tt}_2Zr(\mu\text{-}S)_2Ir(CO)_2Rh(cod)_2]$ (2.8205(10) Å; $Cp^{tt}=\eta^5$-1,3-di-*tert*-butylcyclopentadienyl)[10] (with a μ-S-supported metal–metal bond) and in the heterodinuclear cations $[RhIr(CH_3)(CO)_3(\mu\text{-}dppm)_2]^+$ (2.743(1) Å),[11] and $[RhIr(CO)_3(\mu\text{-}dppm)_2]^+$ (2.7722(7) Å).[12] Longer metal–metal distances were observed in the cluster $[(Cp^*Ir)_2(\mu_3\text{-}S)_2Rh(cod)][RhCl_2(cod)]$ (2.906(1) Å and 2.913(9) Å).[13] The presence of a d^8–d^8 Rh(1)–Ir(2) interaction in **3** is also supported by the Rh(1)-S-Ir(2) angles (69.59(18)° and 69.8(2)°), that are smaller than the Rh(1)-S-Ir(1) angles (79.5(2)° and 80.3(2)°).

Reaction of $[Cp^*Ir\{S_2C_2(B_{10}H_{10})\}]$ (1a) with $[\{Rh(cod)(\mu\text{-}Cl)\}_2]$ in the ratio of 1:1: We prepared the dinuclear complex $[Rh_2(cod)_2\{(\mu\text{-}SH)(\mu\text{-}SC)(CH)(B_{10}H_{10})\}]$ (**4**) by refluxing a solution containing both $[Cp^*IrS_2C_2(B_{10}H_9)]$ (**1a**) and $[\{Rh(cod)(\mu\text{-}Cl)\}_2]$ (1:1) in toluene. The complex **4** was isolated as an orange-red air-stable solid. The ^{1}H NMR spectrum of **4** exhibits a carborane (C↔H) resonance at $\delta=5.31$ and an S↔H resonance at $\delta=0.86$ ppm.

The X-ray diffraction analysis of the structure of molecule **4** confirms a dinuclear rhodium(I) thiolate complex; the molecular structure is shown in Figure 3 and selected structural data are given in Table 3. The structure differs from that of $[Rh_2(cod)_2\{S_2C_2(B_{10}H_{10})\}]$, which had been synthesized by the reaction of $[\{Rh(cod)(\mu\text{-}Cl)\}_2]$ with $Li_2S_2C_2(B_{10}H_{10})$ in THF.[14] Two bridging sulfur atoms and a chelating cyclooctadiene are ligated to each metal atom. The dihedral angle along the Rh(1)···Rh(2) vector, between the two planes defined by Rh(1)-Rh(2)-S(1) and Rh(1)-Rh(2)-S(2), is 126.0°. The bond Rh(1)–Rh(2) (3.0213(13) Å) is slightly longer than the intermetallic distances found in the dimers $[\{Rh(\mu\text{-}S(CH_2)_3NMe_2)(cod)\}_2]$ (2.960(1) Å),[15] $[\{Rh(\mu\text{-}SC_6F_5)(cod)\}_2]$ (2.955 Å),[16] and $[\{Rh(\mu\text{-}SC_6F_5)(CO)_4\}_2]$ (2.960 Å).[17] The S(1)–C(1) separation is 1.790(11) Å, which can be compared with the C–S separation in $[Rh_2(cod)_2\{S_2C_2(B_{10}H_{10})\}]$.[14] On the other hand, the S(2)–C(2) bond is cleaved and the distance is 3.354 Å. The Rh–S bond lengths, 2.359(3)–2.425(6) Å, are statistically slightly different, but compare well with those found in the closely related μ_3-sulfido Rh–Rh complex $[Cp(acac)Ti(\mu_3\text{-}S)_2\{Rh(cod)_2\}]$ (2.3333(7)–2.3419(7) Å),[18] and in the tetranuclear cluster $[Rh_4(\mu\text{-}PyS_2)_2(cod)_4]$ (2.391–2.394(1) Å).[19] The Rh–C bond lengths in complex **4** fall in the range of 2.073(11)–2.158(11) Å, and are similar to those in complex **2**.

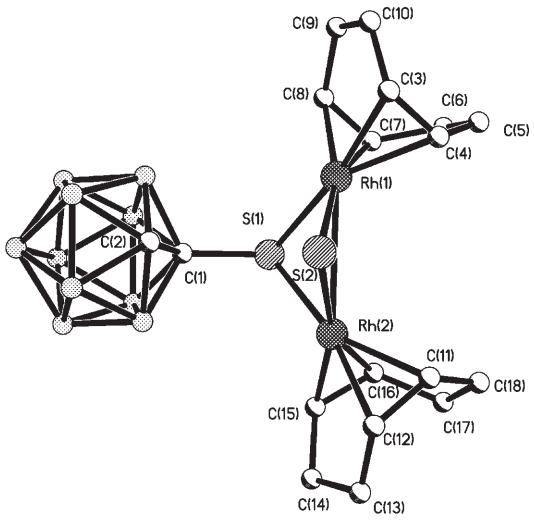

Figure 3. Molecular structure of dinuclear rhodium complex **4** with atom labelling, all hydrogen atoms are omitted for clarity.

Table 3. Selected bond lengths [Å] and angles [°] for the dinuclear rhodium complex **4**.

Rh(1)–S(1)	2.359(3)	Rh(1)–S(2)	2.425(6)
Rh(1)–C(3)	2.158(11)	Rh(1)–C(4)	2.144(12)
Rh(1)–C(7)	2.122(11)	Rh(1)–C(8)	2.105(10)
Rh(1)–Rh(2)	3.0213(13)	S(1)–C(1)	1.790(11)
Rh(2)–S(1)	2.375(3)	Rh(2)–S(2)	2.405(5)
Rh(2)–C(11)	2.153(11)	Rh(2)–C(12)	2.148(11)
Rh(2)–C(15)	2.073(11)	Rh(2)–C(16)	2.098(11)
C(1)–C(2)	1.638(15)		
Rh(1)-S(1)-Rh(2)	79.34(9)	Rh(1)-S(2)-Rh(2)	77.45(14)
Rh(1)-S(1)-C(1)	112.5(3)	Rh(2)-S(1)-C(1)	110.9(3)
S(1)-Rh(1)-Rh(2)	50.57(7)	S(2)-Rh(1)-Rh(2)	50.98(12)
S(1)-Rh(2)-Rh(1)	50.10(7)	S(1)-C(1)-C(2)	123.8(8)
S(1)-Rh(2)-S(2)	87.47(16)	S(1)-Rh(1)-S(2)	87.37(13)

Reaction of $[Cp^*Ir\{S_2C_2(B_{10}H_{10})\}]$ (1a) with $[W(CO)_3(py)_3]$ (py = pyridine, NC_5H_5): Compound **1a** reacts with $[W(CO)_3(py)_3]$ (py = pyridine, NC_5H_5) in the presence of more than three equivalents of BF_3 in diethyl ether to give the mixture of complexes **5**–**7** (Scheme 3). This is different with $[Mo(CO)_3(py)_3]$ reactions. At room temperature, compound **5** is formed in much lower quantities, whereas the major products are complexes **6** and **7**. We did not obtain compound **5** at room temperature.[5c] We achieved high-yield formation of **5** by refluxing the mixture in toluene for 12 h; during this procedure the solution turned dark red, from which we obtained a dark red prismatic crystal after chromatography on silica gel and recrystallization from toluene/hexane. We characterized compound **5** by using elemental analyses and X-ray diffraction studies (selected structural data are given in Table 4).

The IR spectrum of **5** (KBr pellet) shows two strong absorptions at 1832 and 1790 cm^{-1}. Based on information obtained from the X-ray diffraction study, we attributed these bands to the absorption pattern of bridging CO groups of the $[Ir_2W(CO)_2]$ fragment. The ^{1}H NMR spectra exhibit only one singlet attributed to the methyl groups of the Cp* ring. The crystal structure of **5** consists of the $Ir_2W(CO)_2$ backbone that is bridged by two *o*-carborane-1,2-dithiolato ligands and capped by two Cp* rings. The two Ir–W single bonds (2.7445(7) and 2.7851(6) Å), which are each supported by a symmetrically bridging *o*-carborane dithiolato ligand, may therefore be compared with the corresponding bonds in sulfido-bridged Ir–W complexes such as $[Ir(PPh_3)_2(\mu_3\text{-}S)(\mu_2\text{-}S)_3\{W(S_2CNEt_2)\}_2(\mu_2\text{-}Cl)]$ (2.859(2) and 2.878(2) Å),[20] and $[(Me_2Tp)W(\mu\text{-}S)_3IrCp^*][PF_6]$

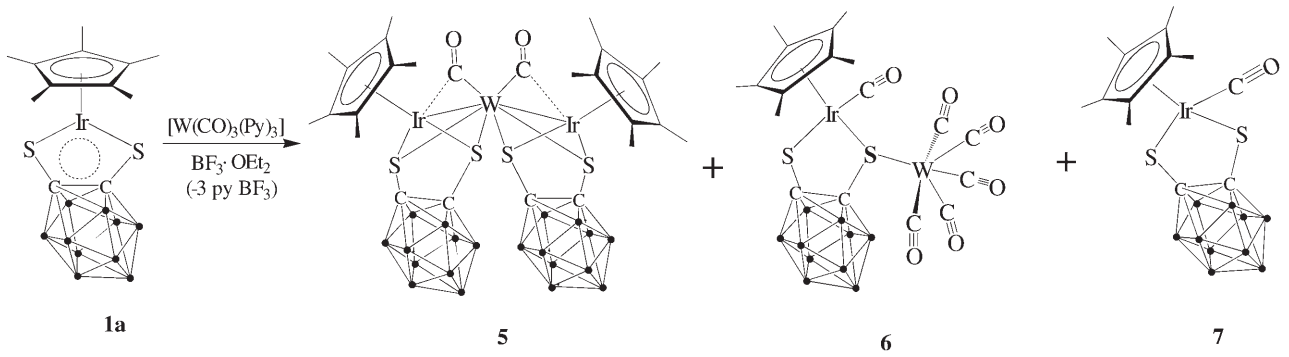

Scheme 3. Reaction of iridium complex **1a** with $[W(CO)_3(py)_3]$ to give complexes **5**, **6**, and **7**.

Table 4. Selected bond lengths [Å] and angles [°] for **5**.

Ir(1)–W(1)	2.7851(6)	Ir(1)–C(5)	2.498(9)
Ir(1)–S(1)	2.339(2)	Ir(1)–S(2)	2.400(2)
C(1)–C(2)	1.641(12)	W(1)–S(1)	2.543(2)
W(1)–S(2)	2.531(2)	W(1)–C(5)	1.947(9)
C(5)–O(1)	1.180(10)	W(1)–C(6)	1.971(9)
C(6)–O(2)	1.157(10)	W(1)–S(3)	2.504(2)
W(1)–S(4)	2.554(2)	Ir(2)–W(1)	2.7445(7)
Ir(2)–C(6)	2.586(9)	Ir(2)–S(3)	2.340(2)
Ir(2)–S(4)	2.390(2)	C(3)–C(4)	1.613(11)
Ir(1)-S(1)-C(1)	103.5(3)	Ir(1)-S(2)-C(2)	104.5(3)
Ir(1)-W(1)-S(1)	51.83(5)	Ir(1)-S(1)-W(1)	69.43(6)
S(1)-Ir(1)-S(2)	79.71(7)	Ir(1)-W(1)-Ir(2)	145.171(16)
W(1)-C(5)-O(1)	162.4(7)	W(1)-C(6)-O(2)	165.9(8)
Ir(2)-S(3)-W(1)	68.92(6)	Ir(2)-W(1)-S(3)	52.72(5)
S(3)-Ir(2)-S(4)	79.58(7)		

(2.6415(6) Å).[21] The Ir–S bond lengths in molecule **5** (2.339(2)–2.400(2) Å) are close to those in complexes **2** and **3**. The planar pseudoaromatic system of the iridadithiolate heterocycle **1a** is no longer present in molecule **5**; the dihedral angles at the S···S vector in the IrS_2C_2 rings are 133.3° and 132.6°, respectively. The structure of molecule **5** is depicted in Figure 4.

Reaction of $[Cp^*Rh\{S_2C_2(B_{10}H_{10})\}]$ (1b) with $[\{Rh(cod)(\mu\text{-}Cl)\}_2]$: To gain further insight into the reaction of 16-electron complexes with low-valence metal complexes, we prepared and studied analogous rhodium complexes **1b** with a similar structure to **1a**. They all have unsaturation properties at the metal and sulfur atoms. Reactions of **1b** with $[\{Rh(cod)(\mu\text{-}Cl)\}_2]$ in THF gave the *cis* and *trans* isomers **8** and **9**. In refluxing THF solution, the cisoid **8** was converted in more than 95% yield to the transoid **9**, which did not contain a boron–iridium bond like the corresponding iridium complex **3** (Scheme 4).

The molecular structures of isomers **8** and **9** are shown in Figure 5 and Figure 6, respectively. In the two complexes, the rhodium atoms of the Cp*Rh fragment have been reduced from Rh^{III} to Rh^{II}, apparently by $[\{Rh^{I}(cod)(\mu\text{-}Cl\}_2]$. The molecule **8** contains a C_2 axis. The Rh–Rh lengths in **8** (2.6460(7) Å) may therefore be compared with the Ir–Rh lengths in the analogous trinuclear complex *cis*-$[\{Cp^*Ir[Se_2C_2(B_{10}H_{10})]\}_2Rh]$ (2.7097(11), 2.6630(11) Å)[5a](see

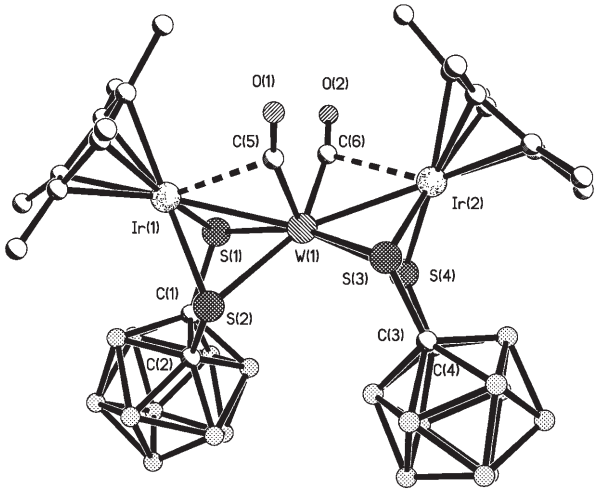

Figure 4. Molecular structure of complex **5** with atom labelling, all hydrogen atoms are omitted for clarity.

Table 5). In isomer **9**, the *o*-carborane groups are drawn sufficiently close to the rhodium center with the distance of Rh(1)···B(3) being 3.162 Å (3.377 Å in **8**). It should be noted that the cyclometalated reaction did not occur. In contrast with **8**, the Rh–Rh length (2.8232(11) Å) has increased in **9**, and is due to the inducement of the metal atom to the neighbor borane atom in the carborane. This

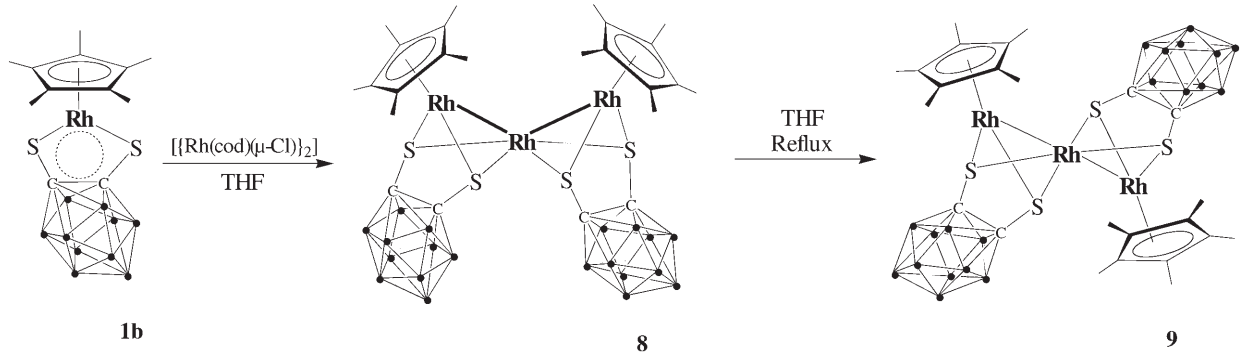

1b 8 9

Scheme 4. Synthesis of complexes **8** and **9**.

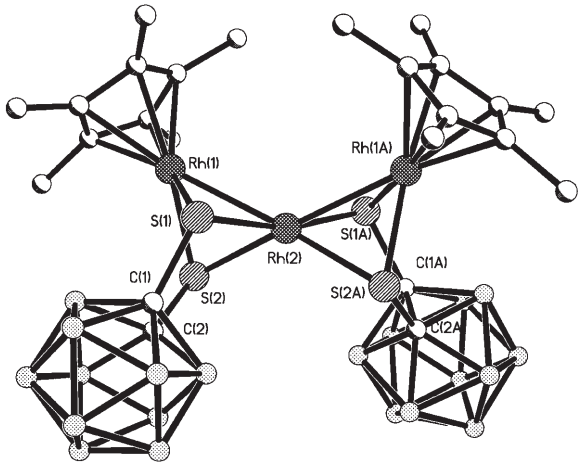

Figure 5. Molecular structure of complex **8** with atom labelling, all hydrogen atoms are omitted for clarity.

Table 5. Selected bond lengths [Å] and angles [°] for **8** and **9**.

Complex **8**		Complex **9**	
Rh(1)–S(1)	2.3650(14)	Rh(1)–S(1)	2.371(4)
Rh(1)–S(2)	2.3465(14)	Rh(1)–S(2)	2.369(4)
Rh(1)–Rh(2)	2.6460(7)	Rh(1)–Rh(2)	2.8232(11)
C(1)–C(2)	1.628(7)	C(1)–C(2)	1.629(16)
Rh(2)–S(1)	2.3458(15)	Rh(2)–S(1)	2.318(5)
Rh(2)–S(2)	2.4222(14)	Rh(2)–S(2)	2.315(5)
S(1)–C(1)	1.822(5)	S(1)–C(1)	1.800(14)
S(2)–C(2)	1.811(5)	S(2)–C(2)	1.788(14)
Rh(1)-S(1)-Rh(2)	68.34(4)	Rh(1)-S(1)-Rh(2)	74.03(11)
Rh(1)-S(2)-Rh(1)	67.38(4)	Rh(1)-S(2)-Rh(1)	74.12(11)
Rh(1)-S(1)-C(1)	103.40(17)	Rh(1)-S(1)-C(1)	94.2(4)
Rh(1)-S(2)-C(2)	103.81(16)	Rh(1)-S(2)-C(2)	94.2(4)
Rh(2)-S(1)-C(1)	104.17(16)	Rh(2)-S(1)-C(1)	104.1(4)
Rh(2)-S(2)-C(2)	102.60(16)	Rh(2)-S(2)-C(2)	102.8(4)
S(1)-Rh(1)-S(2)	80.51(5)	S(1)-Rh(1)-S(2)	80.52(14)
S(1)-Rh(2)-S(2)	79.34(5)	S(1)-Rh(2)-S(2)	82.78(16)
Rh(1)-Rh(2)-Rh(1A)	127.87(3)	Rh(1)-Rh(2)-Rh(1A)	180.0

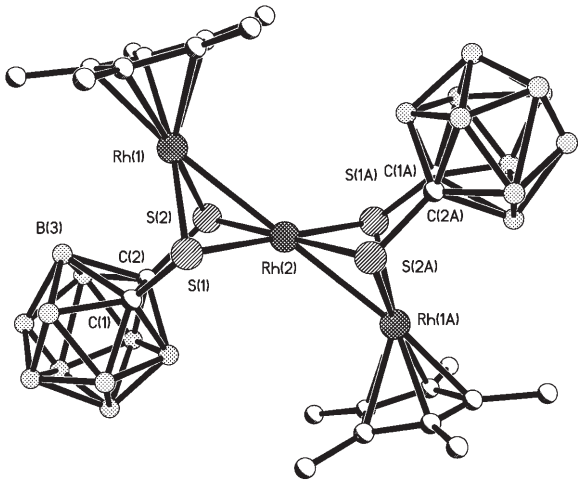

Figure 6. Molecular structure of complex **9** with atom labelling, all hydrogen atoms are omitted for clarity.

effect can also be noted in the change of dihedral angle at the S(1)···S(2) vector in the RhS_2C_2 ring (118.3°), in contrast to 133.9° in isomer **8**. In complex **3**, this dihedral angle is 105.6 at the S(1)···S(2) vector in the IrS_2C_2 ring containing the Ir–B bond segment. All these prove the presence of metal-induced B–H activation effects in the formation of isomer **9**.

Conclusion

This work focused on the formation of clusters containing heteronuclear metal–metal bonds, which are supported by bridging 1,2-dicarba-*closo*-dodecaborane(12)-1,2-dithiolato ligands. The dinuclear half-sandwich complex **2**, the trinuclear complex **3**, and the dinuclear complex **4** were all obtained in the course of the reactions of the 16-electron half-sandwich complex **1a** with $[\{Rh(cod)(\mu\text{-}Cl)\}_2]$ under different reaction conditions. Complex **3** was synthesized in refluxing toluene either by the reaction of complex **1a** with $[\{Rh(cod)(\mu\text{-}Cl)\}_2]$ in the molar ratio 4:1, or by the reaction of complex **1a** with **2** in the molar ratio 1:1. The ancillary o-carborane-1,2-dithiolato ligands played a key role in determining the kind of products formed. In addition, firm evidence of metal-induced B–H activation was provided by the presence of new iridium–boron bonds in the complexes **2** and **3**. Furthermore, a rational synthesis route to trinuclear

complex **5** was established through the reaction of **1a** with $[W(CO)(py)_3]$ in the presence of excess $BF_3{\cdot}Et_2O$. The formation of mixed metal–metal bonds in complexes **2, 3**, and **5** during the reaction of the 16-electron complex **1a** involved redox processes, during which iridium was partially reduced by low-valence transition-metal complexes such as the fragments [Rh(cod)(μ-Cl)] or $[W(CO)_3]$. Thus, the reaction of the mononuclear iridium dithiolato complex **1a** with low-valent metal complexes has been proved to be a convenient synthetic route for the construction of new heteronuclear complexes having [IrRh], $[Ir_2Rh]$, or $[Ir_2W]$ cores. Further investigations prove that the analogous system of complex **1b** also can be used to synthesize trinuclear complexes containing a $[Rh_3]$ core through the reactions with $[\{Rh(cod)(\mu\text{-}Cl)\}_2]$. The *cis* and *trans* isomers **8** and **9** are structurally slightly different than the analogous complexes **3** obtained through the same route which proved be useful in **1a**.

Compared with the metal–metal bonds in the Ir_2Rh and Rh_3 complexes, the Ir–Rh, Rh–Rh separations are in the same range when they adopt the *cis* structure. During the formation of the transoid structure, the separation between the metal atoms increases. In the *trans* isomers of Rh_3 complexes, the Rh–Rh lengths are still in the normal range of a metal bond. While, in *trans* Ir_2Rh complexes, one of the metal–metal bonds of Ir–Rh was longer than before, a fact that can be explained by the difference of the formal oxidation ("valence") state in *trans*-Ir_2Rh and -Rh_3.

Experimental Section

All manipulations were performed under an atmosphere of nitrogen using standard Schlenk techniques. Solvents were dried by refluxing over sodium/benzophenone ketyl (toluene, hexane, cyclohexane) and were distilled just before use. $[Cp^*Ir\{S_2C_2(B_{10}H_{10})\}]$ (**1a**),[6] $[Cp^*Rh\{S_2C_2(B_{10}H_{10})\}]$ (**1b**),[3] $[\{Rh(cod)(\mu\text{-}Cl)\}_2]$,[22] and $[W(CO)_3(py)_3]$[23] were prepared by methods reported previously. IR spectra were recorded on a Nicolet AVATAR-360IR spectrometer, whereas ^1H (500 MHz), ^{11}B (160 MHz), and ^{13}C (125 MHz) NMR spectra were obtained on a Bruker DMX-500 spectrometer in $CDCl_3$ solution. Elemental analyses were performed on an Elementar Vario EI Analyzer.

Synthesis of $[\{Cp^*Ir[S_2C_2(B_{10}H_9)]\}Rh(cod)]$ (2): A solution of $[\{Rh(cod)(\mu\text{-}Cl)\}_2]$ (50 mg, 0.1 mmol) in toluene (15 mL) was added to a suspension of **1a** (106 mg, 0.2 mmol) in toluene (30 mL). The deep blue mixture was heated under reflux for two days, and thereby gradually changed to dark red. The solvent was then evaporated under vacuum, and the components of the residue were separated by column chromatography on silica using hexane/toluene (4:1 v/v) for elution. The first red band was isolated and the residue recrystallized from benzene/hexane to give red crystals of complex **2** (91 mg, 61%). ^1H NMR(500 MHz, $CDCl_3$): $\delta = 2.11$ (s, 15H; C_5Me_5), 2.49 (br, 8H; cod(CH_2)), 4.23 ppm (s, 4H; cod(CH=)); ^{11}B NMR(160 MHz, $CDCl_3$): $\delta = -3.6$, -6.2, -9.4, -10.6, -12.4, -18.9 ppm (Ir–B) (in the ratio 1:2:2:2:2:1); ^{13}C NMR(125 MHz, CD_3Cl): $\delta = 10.1$ (s, Cp*(Me)), 29.7 and 32.8 (s, CH_2), 77.2 (s, C_2-carborane), 89.5 (d, $=CH_2$), 103.2 ppm (s, Cp*); IR (KBr pellet): $\tilde{\nu} = 2570$ (ν(B–H)) cm^{-1}; elemental analysis (%) calcd for $C_{20}H_{36}B_{10}S_2IrRh$: C 32.29, H 4.88; found: C 32.01, H 4.79.

Synthesis of *trans*-$[\{Cp^*Ir[S_2C_2(B_{10}H_9)]\}Rh\{[S_2C_2(B_{10}H_{10})]IrCp^*\}]$ (3): *Method A*: $[Rh(cod)(\mu\text{-}Cl)]_2$ (25 mg, 0.05 mmol) was added to a solution of **1a** (106 mg, 0.2 mmol) in toluene (30 mL) at room temperature. The deep blue suspension was refluxed for two days, and thereby the solution gradually changed to dark red. The solvent was then evaporated under vacuum, and the components of the residue were separated by column chromatography on silica. The component in the first band was eluted with toluene/hexane (1:4 v/v) and was recrystallized from toluene/hexane at −18°C to give dark red crystals of compound **3** (66 mg, 56%). ^1H NMR (500 MHz, $CDCl_3$): $\delta = 2.11$ (s, 15H; C_5Me_5), 2.19 ppm (s, 15H; C_5Me_5); ^{11}B NMR (160 MHz, $CDCl_3$): $\delta = -4.5$, -6.1, -9.2, -10.4, -12.2, -19.0 ppm (Ir–B) (signals overlap); ^{13}C NMR (125 MHz, $CDCl_3$): $\delta = 8.9$ and 9.3 (s, Cp*(Me)), 76.7 and 77.1 (s, C_2-carborane), 101.0 and 103.2 ppm (s, Cp*); IR (KBr pellet): $\tilde{\nu} = 2558$ (ν(B–H)) cm^{-1}; elemental analysis (%) calcd for $C_{24}H_{49}B_{20}S_4Ir_2Rh$: C 24.65, H 4.22; found: C 24.38, H 4.16. *Method B*: An equimolar mixture of **1a** (53 mg, 0.1 mmol) and **2** (75 mg, 0.1 mmol) in toluene (30 mL) was refluxed for 20 h. After evaporation of the solvent, the residue was separated by column chromatography on silica. The first band, eluted with toluene/hexane (1:4 v/v), contained complex **3** (70 mg, 60%).

Synthesis of $[Rh_2(cod)_2\{S(SH)C(CH)(B_{10}H_{10})\}]$ (4): A solution of $[\{Rh(cod)(\mu\text{-}Cl)\}_2]$ (50 mg, 0.1 mmol) in toluene (15 mL) was added to a suspension of **1a** (53 mg, 0.1 mmol) in toluene (30 mL). The deep blue mixture was refluxed for two days, and thereby gradually changed to dark red. After evaporation of the solvent and chromatography on silica (elution with CH_2Cl_2/hexane 1:4 v/v), the first orange band was isolated and the residue was recrystallized from benzene/hexane to give orange-red crystals of compound **4** (37 mg, 58%). ^1H NMR (500 MHz, $CDCl_3$): $\delta =$ 0.86 (s, 1H; S–H), 1.89 (m, 4H; cod(CH_2)), 1.97 (m, 4H; cod(CH_2)), 2.11 (m, 4H; cod(CH_2)), 2.48(m, 4H; cod(CH_2)), 4.23 (s, 4H; cod(CH=)), 4.68 (s, 4H; cod(CH=)), 5.31 ppm (s, 1H; carborane(C–H)); ^{11}B NMR (160 MHz, $CDCl_3$): $\delta = -2.2$, -6.1, -9.4, -12.5, -13.8 ppm (in the ratio 2:3:1:3:1); ^{13}C NMR (125 MHz, $CDCl_3$): $\delta = 31.9$ and 32.5 (s, CH_2), 65.0 and 67.8 (s, $=CH_2$), 76.8 and 77.3 ppm (s, C_2-carborane); IR (KBr pellet): $\tilde{\nu} = 2556$ (ν(B–H)) cm^{-1}; elemental analysis (%) calcd for $C_{18}H_{36}B_{10}S_2Rh_2$: C 34.29, H 5.75; found: C 34.17, H 5.62.

Synthesis of complexes 5–7: $BF_3{\cdot}OEt_2$ (0.26 mL, 47%, 1.0 mmol) was added dropwise at room temperature to a mixture of **1a** (106 mg, 0.20 mmol) and $[W(CO)_3(py)_3]$ (51 mg, 0.10 mmol) in toluene (20 mL). The deep blue suspension was refluxed for 12 h, during which time the color became deep red. The solvent was then removed under vacuum, and the components of the residue were separated by column chromatography on silica. The first band was eluted with toluene/hexane (1:4 v/v) and the product was recrystallized from toluene/hexane at −18°C to give orange crystals of compound **6** (18 mg, 10%). Compound **6**: ^1H NMR (500 MHz, $CDCl_3$): $\delta = 1.90$ ppm (s, 15H; C_5Me_5); IR (KBr pellet): $\tilde{\nu} =$ 2570 (ν(B–H)); 2073, 2040, 1987, 1926, 1905 (ν(CO)) cm^{-1}; elemental analysis(%) calcd for $C_{18}H_{25}B_{10}IrO_6S_2W$: C 24.41, H 2.85; found: C 24.26, H 2.77. The component in the second chromatography band was recrystallized from toluene/hexane to afford deep red crystals of compound **5** (67 mg, 51%). Compound **5**: ^1H NMR (500 MHz, $CDCl_3$): $\delta = 1.91$ ppm (s, 30H; C_5Me_5); ^{11}B NMR (160 MHz, $CDCl_3$): $\delta = -4.8$, -6.3, -7.9, -12.3 ppm (in the ratio 2:2:2:4); ^{13}C NMR (125 MHz, $CDCl_3$): $\delta = 8.9$ (s, Cp*(Me)), 78.9 (s, C_2-carborane), 101.8 (s, Cp*), 172.0 ppm (s, CO); IR (KBr pellet): $\tilde{\nu} = 2593$ (ν(B–H)), 1832 and 1790 cm^{-1} (ν(CO)); elemental analysis(%) calcd for $C_{26}H_{50}B_{20}Ir_2O_2S_4W$: C 23.88, H 3.85; found: C 23.61, H 3.73. The complex **7** was eluted with CH_2Cl_2/hexane (1:3 v/v). Recrystallization from toluene/hexane at −18°C gave yellow-green crystals of **7** (6 mg, 6%). ^1H NMR (500 MHz, $CDCl_3$): $\delta = 1.91$ ppm (s, 15H; C_5Me_5); IR (KBr pellet): $\tilde{\nu} = 2563$ (ν(B–H)), 2038 cm^{-1} (ν(CO)); elemental analysis(%) calcd for $C_{13}H_{25}B_{10}IrOS_2$: C 27.79, H 4.49; found: C 27.50, H 4.31.

Synthesis of *cis*- and *trans*-$[\{Cp^*Rh[S_2C_2(B_{10}H_{10})]\}_2Rh]$ (8, 9): $[\{Rh(cod)(\mu\text{-}Cl)\}_2]$ (50 mg, 0.1 mmol) was added to the green solution containing complex **1b** (178 mg, 0.4 mmol) in THF (30 mL). The mixture was stirred for 8 h and the color changed from green to violet. After removal of the solvent, the residue was subjected to chromatography on silica gel. Elution with hexane gave complex **9** (79 mg, 39%) as a violet zone. Recrystallization from hexane afforded air-stable dark-violet crystals. ^1H NMR (500 MHz, $CDCl_3$): $\delta = 2.02$ ppm (s, 30H; C_5Me_5); ^{11}B NMR (160 MHz, $CDCl_3$): $\delta = -5.6$, -7.6 -8.9, -10.7, -14.6, -16.2 ppm (signals overlap); IR(KBr disk): $\tilde{\nu} = 2572$ (ν(B–H)) cm^{-1}; elemental analysis (%) calcd for $C_{24}H_{50}B_{20}S_4Rh_3$: C 29.06, H 5.08; found: C 28.99, H 5.07. The second

dark red chromatography zone was close to the first band. Elution with toluene/hexane (1:10 v/v) as a dark red band. Recrystallization from benzene/hexane afforded red crystals of **8** (50 mg, 25%). ^{1}H NMR (500 MHz, $CDCl_3$): $\delta = 1.86$ ppm (s, 30H; C_5Me_5); ^{11}B NMR (160 MHz; $CDCl_3$): $\delta = -4.5, -6.2, -8.1, -10.3$ ppm (in the ratio 2:2:2:4); IR (KBr disk): $\tilde{\nu} = 2563$, 2586 cm^{-1}(B–H); elemental analysis (%) calcd for $C_{24}H_{50}B_{20}S_4Rh_3$: C 29.06, H 5.08; found: C 28.77, H 4.89.

Crystallographic analysis: Dark red crystals of **2–5, 8,** and **9** were grown by slow diffusion from toluene/hexane or benzene/hexane mixtures. The selected crystals were mounted by gluing onto the end of a thin glass fiber. X-ray intensity data were collected on the CCD-Bruker SMART APEX system. The determination of the unit cell and the collection of intensity data were performed with graphite-monochromated $Mo_{K\alpha}$ radiation ($\lambda = 0.71073$ Å). All the data were collected at room temperature using the ω scan technique. The structures were solved by direct methods, using Fourier techniques, and refined on F^2 by a full-matrix least-squares method. All non-hydrogen atoms were refined with anisotropic thermal parameters. The hydrogen atoms were included but not refined. All the calculations were carried out using the program SHELXTL. Crystal data, data collection parameters, and the results of the analyses of compounds **2–5**, **8**, and **9** are listed in Table 6 and Table 7. CCDC-258748 (**2**), CCDC-258746 (**3**), CCDC-258749 (**4**), CCDC-258747 (**5**), CCDC-276920 (**8**), and CCDC-276921 (**9**) contain the supplementary crystallographic data for this paper. These data can be obtained free of charge from the Cambridge Crystallographic Data Centre via www.ccdc.cam.ac.uk/data_request/cif.

Table 6. Crystallographic data for compounds **2–4**.

	2	**3**	**4**
empirical formula	$C_{20}H_{36}B_{10}S_2IrRh$	$C_{24}H_{49}B_{20}S_4Ir_2Rh$	$C_{18}H_{36}B_{10}S_2Rh_2$
M_r	743.82	1169.38	630.51
crystal size [mm^3]	0.30×0.05×0.05	0.05×0.04×0.04	0.10×0.05×0.05
crystal system	orthorhombic	monoclinic	orthorhombic
space group	*Pnma*	*P*2(1)/*n*	*Pbca*
a [Å]	18.089(6)	10.172(4)	11.290(3)
b [Å]	12.779(4)	13.109(5)	13.340(4)
c [Å]	12.051(4)	16.521(6)	34.051(9)
β [°]		105.580(6)	
V [Å^3]	2785.6(15)	2122.1(14)	5128(2)
Z	4	2	8
ρ_{calcd} [g cm^{-3}]	1.774	1.830	1.633
$\mu(Mo_{K\alpha})$ [mm^{-1}]	5.524	6.857	1.457
collected reflns	12322	9486	20403
unique reflns	2858	7784	4519
parameters	173	474	307
goodness-of-fit	1.089	1.076	1.008
R_1[a] ($I > 2\sigma(I)$)	0.0358	0.0781	0.0651
wR_2[a] ($I > 2\sigma(I)$)	0.0901	0.1457	0.1220
max/min residual density [e Å^{-3}]	1.223/−0.981	2.306/−1.550	1.433/−0.598

[a] $R_1 = \Sigma||F_o| - |F_c||$ (based on reflections with $F_o^2 > 2\sigma F^2$). $wR_2 = [\Sigma[w(F_o^2 - F_c^2)^2]/\Sigma[w(F_o^2)^2]]^{1/2}$; $w = 1/[\sigma^2(F_o^2) + (0.095P)^2]$; $P = [\max(F_o^2, 0) + 2F_c^2]/3$ (also with $F_o^2 > 2\sigma F^2$).

Table 7. Crystallographic data for compounds **5**, **8**, and **9**.

	5	**8**	**9**
empirical formula	$C_{26}H_{50}B_{20}O_2S_4Ir_2W$	$C_{24}H_{50}B_{20}S_4Rh_3 \cdot C_6H_6$	$C_{24}H_{50}B_{20}S_4Rh_3$
M_r	1307.35	1069.92	991.81
crystal size [mm^3]	0.15×0.15×0.04	0.18×0.10×0.10	0.10×0.08×0.05
crystal system	monoclinic,	monoclinic	monoclinic
space group	*P*2(1)/*c*	*C*2/*c*	*P*2(1)/*n*
a [Å]	14.048(3)	12.091(3)	10.140(3)
b [Å]	21.312(5)	23.116(6)	13.078(3)
c [Å]	15.405(4)	18.064(5)	16.582(4)
β [°]	109.822(4)	103.587(4)	105.711(4)
V [Å^3]	4338.7(17)	4907(2)	2116.8(10)
Z	4	4	2
ρ_{calcd} [g cm^{-3}]	2.001	1.448	1.556
$\mu(Mo_{K\alpha})$ [mm^{-1}]	8.985	1.191	1.374
collected reflns	19883	10229	8687
unique reflns	8538	4334	3723
parameters	516	258	247
goodness-of-fit	0.982	0.926	1.141
R_1[a] ($I > 2\sigma(I)$)	0.0414	0.0362	0.0944
wR_2[a] ($I > 2\sigma(I)$)	0.0740	0.0878	0.1678
max/min residual density [e Å^{-3}]	1.364/−0.903	0.776/−0.407	1.218/−1.681

[a] $R_1 = \Sigma||F_o| - |F_c||$ (based on reflections with $F_o^2 > 2\sigma F^2$). $wR_2 = [\Sigma[w(F_o^2 - F_c^2)^2]/\Sigma[w(F_o^2)^2]]^{1/2}$; $w = 1/[\sigma^2(F_o^2) + (0.095P)^2]$; $P = [\max(F_o^2, 0) + 2F_c^2]/3$ (also with $F_o^2 > 2\sigma F^2$).

Acknowledgements

Financial support by the National Science Foundation of China for Distinguished Young Scholars (29925101, 20421303), and by the Special Funds for Major State Basic Research Projects (1999064800) is gratefully acknowledged.

[1] a) G.-X. Jin, *Coord. Chem. Rev.* **2004**, *248*, 587–602; b) G.-X. Jin in *Perspectives in Organometallic Chemistry* (Eds.: C. G. Screttas, B. R. Steele), RSC Cambridge Press, **2003**, pp. 47–61.
[2] a) D. H. Kim, J. Ko, K. Park, S. Cho, S. O. Kang, *Organometallics* **1999**, *18*, 2738–2740; b) X.-F. Hou, X.-C. Wang, J.-Q. Wang, G.-X. Jin, *J. Organomet. Chem.* **2004**, *689*, 2228–2235.
[3] a) M. Herberhold, G.-X. Jin, H. Yan, W. Milius, B. Wrackmeyer, *J. Organomet. Chem.* **1999**, *587*, 252–257; b) J. Y. Bae, Y. I. Park, J. Ko, K. I. Park, S. I. Cho, S. O. Kang, *Inorg. Chim. Acta* **1999**, *289*, 141–148.
[4] a) M. Herberhold, H. Yan, W. Milius, B. Wrackmeyer, *Angew. Chem.* **1999**, *111*, 3888–3890; *Angew. Chem. Int. Ed.* **1999**, *38*, 3689–3691; b) M. Herberhold, H. Yan, W. Milius, B. Wrackmeyer, *Chem. Eur. J.* **2000**, *6*, 3026–3032; c) M. Herberhold, H. Yan, W. Milius, B. Wrackmeyer, *Chem. Eur. J.* **2002**, *8*, 388–395.
[5] a) G.-X. Jin, J.-Q. Wang, Z. Zhang, L. H. Weng, M. Herberhold, *Angew. Chem.* **2005**, *117*, 264–267; *Angew. Chem. Int. Ed.* **2005**, *44*, 259–262; b) J.-Q. Wang, L.-H. Weng, G.-X. Jin, *J. Organomet. Chem.* **2005**, *690*, 249–252; c) J.-Q. Wang, L.-H. Weng, G.-X. Jin, *Rev. Inorg. Chem.* **2005**, *27*, 55–66; d) J.-Q. Wang, X. Hou, L. H. Weng, G.-X. Jin, *Organometallics* **2005**, *24*, 826–830.
[6] a) M. Herberhold, G.-X. Jin, H. Yan, W. Milius, B. Wrackmeyer, *Eur. J. Inorg. Chem.* **1999**, 873–875; b) Q. Kong, G.-X. Jin, S. Y. Cai, L. H. Weng, *Chin. Sci. Bull.* **2003**, *48*, 1733–1735.
[7] E. L. Hoel, M. F. Hawthorne, *J. Am. Chem. Soc.* **1974**, *96*, 6770.
[8] a) J.-Y. Bae, Y.-J. Lee, S.-J. Kim, J. Ko, S. Cho, S. O. Kang, *Organometallics* **2000**, *19*, 1514–1521; b) Y.-J. Lee, J.-D. Lee, S.-J. Kim, J. Ko, I.-H. Suh, M. Cheong, S. O. Kang, *Organometallics* **2004**, *23*, 135–143.
[9] a) M. T. Pinillos, M. P. Jarauta, L. A. Oro, A. Tiripicchio, M. Tiripicchio-Camellini, *J. Organomet. Chem.* **1988**, *339*, 181–192; b) C. Claver, A. Ruiz, A. M. Masdeu, J. Viñas, T. Saballs, F. J. Lahoz, F. J. Plou, *J. Organomet. Chem.* **1989**, *373*, 269–278; c) K. Tatsumi, H. Kawaguchi, Y. Inoue, A. Nakamura, R. E. Cramer, J. A. Golen, *Angew. Chem.* **1993**, *105*, 791–793; *Angew. Chem. Int. Ed. Engl.* **1993**, *32*, 763–765; d) A. Bisello, A. Ceccon, A. Gambaro, P. Ganis, F. Manoli, S. Santi, A. Venzo, *J. Organomet. Chem.* **2000**, *593*, 315–324; e) A. Ceccon, P. Ganis, F. Manoli, A. Venzo, *J. Organomet. Chem.* **2000**, *601*, 267–270.
[10] M. A. F. Hernandez-Gruel, J. J. Perez-Torrente, M. A. Ciriano, F. J. Lanoz, L. A. Oro. *Angew. Chem.* **1999**, *111*, 2935–2938; *Angew. Chem. Int. Ed.* **1999**, *38*, 2769–2971.
[11] F. H. Antwi-Nsiah, O. Oke, M. Cowie, *Organometallics* **1996**, *15*, 1042–1054.
[12] R. McDonald, M. Cowie, *Inorg. Chem.* **1990**, *29*, 1564–1571.
[13] Z. Tang, Y. Nomura, Y. Ishii, Y. Mizobe, M. Hidai, *Organometallics* **1997**, *16*, 151–154.
[14] S. Y. Cai, X. F. Hou, L.-H. Weng, G.-X. Jin, *J. Organomet. Chem.* **2005**, *690*, 910–915.
[15] A. Polo, C. Claver, S. Castillon, A. Ruiz, J. C. Bayon, J. Real, C. Mealli, D. Masi, *Organometallics* **1992**, *11*, 3525–3533.
[16] C. Cruz-Garritz, B. Rodriguez, H. Torrens, *Transition Met. Chem.* **1984**, *9*, 284–285.
[17] C. Claver, A. M. Masdeu, N. Ruiz, C. Foces-Foces, F. H. Cano, M. C. Apreda, L. A. Oro, J. Garcia-Alejandre, H. Torrens, *J. Organomet. Chem.* **1990**, *398*, 177–186.
[18] M. A. Casado, J. J. Perez-Torrente, M. A. Ciriano, A. J. Edwards, F. J. Lahoz, L. A. Oro, *Organometallics* **1999**, *18*, 5299–5310.
[19] J. J. Perez-Torrente, M. A. Casado, M. A. Ciriano, A. J. Edwards, F. J. Lahoz, L. A. Oro, *Inorg. Chem.* **1996**, *35*, 1782–1791.
[20] T. Ikada, S. Kuwata, Y. Mizobe, M. Hidai, *Inorg. Chem.* **1999**, *38*, 64–69.
[21] H. Seino, N. Iwata, N. Kawarai, M. Hidai, Y. Mizobe, *Inorg. Chem.* **2003**, *42*, 7387–7395.
[22] G. Giordano, R. H. Crabtree, *Inorg. Synth.* **1979**, *19*, 218–220.
[23] a) W. Hieber, F. Muehlbauer, *Z. Anorg. Allg. Chem.* **1935**, *221*, 337–348; b) A. D. Westland, N. Muriithi, *Inorg. Chem.* **1973**, *12*, 2356–2361; c) A. N. Nesmeyanov, V. V. Krivykh, V. S. Kaganovich, M. I. Rybinskaya, *J. Organomet. Chem.* **1975**, *102*, 185–193.

Received: December 24, 2004
Revised: July 8, 2005
Published online: September 27, 2005

